Effect of fluorosubstitution on the structure of single crystals, Effect of fluorosubstitution on the structure of single crystals,thin films and spectral properties of palladium phthalocyanines

SUKJIKH, Aleksander S., KLYAMER, Darya D., PARKHOMENKO, Roman G., KRASNOV, Pavel O., GROMILOV, Sergei A., HASSAN, Aseel <http://orcid.org/0000-0002-7891-8087> and BASOVA, Tamara V.

Effect of fluorosubstitution on the structure of single crystals, thin films and spectral properties of palladium phthalocyanines

Aleksander S. Sukhikh,[a] Darya D. Klyamer,[a] Roman G. Parkhomenko,[a] Pavel O. Krasnov,[a,b]

Sergei A. Gromilov,[a,c] Aseel K. Hassan,[d] Tamara V. Basova[a,c]*[1]

[a]*Nikolaev Institute of Inorganic Chemistry SB RAS, 3, Lavrentieva Ave., 630090 Novosibirsk, Russia*

[b]*Siberian Federal University, 79 Svobodny pr., 660041 Krasnoyarsk, Russia*

[c]*Novosibirsk State University, 2, Pirogova Str., 630090 Novosibirsk, Russia*

[d]*Materials and Engineering Research Institute, Sheffield Hallam University, Sheffield, UK*

Abstract

In this work, the crystalline structure of single crystals grown by vacuum sublimation of unsubstituted palladium phthalocyanines (PdPc), its tetrafluorinated (PdPcF$_4$) and hexadecafluorinated (PdPcF$_{16}$) derivatives have been investigated using X-ray diffraction measurements. Two crystalline phases have been identified for PdPc; the molecules in both phases crystallize in stacks with herringbone arrangement in the monoclinic space groups (C2/c for α-PdPc; P2$_1$/n for γ-PdPc). Both PdPcF$_4$ and PdPcF$_{16}$ crystallize in the triclinic P-1 space group, forming stacks of molecules in columnar arrangement with molecules in adjacent columns are aligned parallel to one another. X-ray diffraction measurements have also been used to elucidate the structural features and molecular orientation of thin films of PdPc, PdPcF$_4$ and PdPcF$_{16}$, grown by organic molecular beam deposition at different substrate temperatures. The effect of fluorosubstitution on UV-visible optical absorption and vibrational spectra of palladium phthalocyanine derivatives is also discussed.

---

[1] Corresponding author: Nikolaev Institute of Inorganic Chemistry SB RAS, 3, Lavrentieva Ave., 630090 Novosibirsk, Russia, tel. +73833308957, fax +73833309489, basova@niic.nsc.ru

1. Introduction

Metal phthalocyanines (MPcs) have received significant interest in applications as active layers of molecular electronic devices due to their remarkable properties, thermal and chemical stability, and performance [1]. Among those MPcs, palladium phthalocyanines (PdPcs) exhibit longer exciton diffusion length in comparison with other bivalent metal phthalocyanines, such as ZnPc and CuPc [2]. This renders them as promising compounds for photovoltaic applications [3-4]. Besides, thin films of palladium phthalocyanine have good sensing properties for different gaseous analytes, with fast response times, high base line stability and enhanced sensitivity. It has recently been shown that PdPc films demonstrate high sensitivity when used as chemical sensors for the detection of oxygen, ammonia, NO_2 and humidity [5-7].

It is known that metal phthalocyanines exhibit rich polymorphism [8], which include the more familiar α- and β-forms, whose packing types are typical for M(II)Pc (M=Zn, Co, Cu, Pd etc.) films. Both polymorphic forms contain stacks of M(II)Pc molecules, which are tilted with respect to the column axis. The angle (θ) between the normal to the ring and the column axis is smaller in the α-form than in the β-form [8]; for instance in the α-CuPc form θ=25.5^o [9], while for β-CuPc θ is 46.5^o [10]. Note that the optical, electrical, sensing and other properties of MPc films comprised of various polymorphic forms may differ significantly and the molecular arrangement of the film may play a crucial role in particular device applications. For example, electronic absorption spectra of α- and β-forms of MPcs are noticeably different [7]. Jafari et al. have reported the strong dependence of sensor response of PdPc films toward ammonia and NO_2 on the phase composition of these films [7].

In contrast to the case of M(II)Pc, much less is known about crystal structure and polymorphic forms of fluorosubstituted M(II)Pcs. Due to the difficulty faced in growing sufficiently large single crystals, previous work on the determination of the crystal structure of $MPcF_{16}$ were contradictory and lack agreement of such parameters as lattice parameter and space group [11-12]. Later on the single crystal structure of micrometre-sized $CuPcF_{16}$ ribbons synthesized by the vaporization–condensation–recrystallization method was resolved by synchrotron X-ray crystallography to have a triclinic unit cell

system [13]. The single crystal polymorph of $CuPcF_{16}$ was found by X-ray diffraction of single crystals to be triclinic, with one molecule per unit cell and parallel (not herringbone) stacking [14]. Single crystal structures of centimeter-sized crystals of $CuPcF_{16}$, $CoPcF_{16}$ and $ZnPcF_{16}$ have also been determined by X-ray diffraction by Jiang et al. [15]. All three derivatives had the $P\bar{1}$ space group, however all crystal structures have been resolved with quite high R-factor (from 12 to 16). To the best of our knowledge, the crystal structure and the polymorphic behavior of fluorinated palladium phthalocyanines have never been studied in the literature.

In this work, the crystal structure of unsubstituted PdPc, its tetrafluorinated $PdPcF_4$ and hexadecafluorinated $PdPcF_{16}$ derivatives (Fig. 1) has been investigated for the first time. Furthermore, the effect of fluorosubstitution on the structure and polymorphic behavior of thin films of palladium phthalocyanines has not been studied before. X-ray diffraction techniques have been used to elucidate the structural features and molecular orientation of thin films of PdPc, $PdPcF_4$ and $PdPcF_{16}$, grown by organic molecular beam deposition. The effect of fluorination on UV-visible optical absorption and vibrational spectra of palladium phthalocyanine derivatives is also discussed.
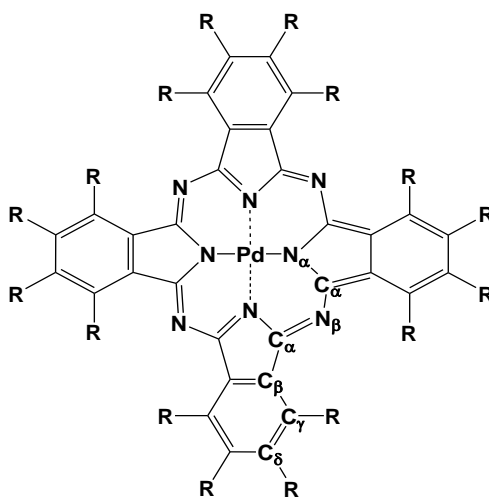

Figure 1. Molecular structure of palladium phthalocyanine derivatives

2. Experimental details

Unsubstituted (PdPc), and hexadecafluorosubstituted ($PdPcF_{16}$) palladium phthalocyanines were synthesized according a procedure described elsewhere [16]. Tetrafluorosubstituted ($PdPcF_4$) palladium

phthalocyanine was synthesized by heating an equimolar 1:4 mixture of palladium chloride with 4-Fluorophthalonitrile (Sigma-Aldrich), in glass tubes for a period of 6-7 hours at 220 $^{\circ}$C. Resulting products were then cleaned from impurities by sublimation in gradient furnace at 450-460° C in glass tube under vacuum (10^{-5} Torr). $PdPcF_4$ was prepared as a statistical mixture of four regioisomers due to the various possible positions of fluorine substituents. No attempt was made to separate the $PdPcF_4$ isomers. The composition of $PdPcF_4$ was investigated in vapour phase by mass spectrometry technique in the temperature range from 300 to 700 $^{\circ}$C. Mass spectra were measured using MI-1201 mass spectrometer. The molecules effusing from the cell were ionized by means of an electron beam of energy 35 eV. MS (m/z): 690.921 (calc. for $C_{32}N_8H_4F_4Pd$ = 690.916 [MPc^+]). Anal. Calc: C, 55.61; H, 1.74; N, 16.22%. Found: C, 51.65; H, 1.71; N, 16.27%. IR spectrum (KBr; ω, cm^{-1}): 3076, 1616, 1541, 1483, 1404, 1329, 1261, 1123, 1055, 957, 867, 820, 746.

To grow single crystals, a small amount of PdPc, $PdPcF_4$ and $PdPcF_{16}$ polycrystalline powders were sealed in a glass ampoule under vacuum (residual pressure ~$2 \cdot 10^{-5}$ Torr) and then sublimed in a gradient furnace at 440-450° C for 2 hours.

Thin films of palladium phthalocyanines were deposited on borosilicate glass slides by two methods. In the first case, films were deposited by organic molecular beam deposition under vacuum of 10^{-5} Torr with the deposition rate of 0.6 nm·s^{-1}. The nominal thickness of the films was about 120 nm. Since substrate temperature did not exceed 50°C during the deposition process, thereafter, those samples will be referred to as the ones deposited onto a "cold substrate". Second set of samples was obtained by vacuum sublimation (10^{-5} Torr) of the respective palladium phthalocyanine powder in a gradient furnace; borosilicate glass substrates were placed at the same position of the ampoule where phthalocyanine single crystals grow during sublimation process. Such an approach yields thin film samples deposited at conditions close to the conditions of the single crystal growth. In this case, the substrate temperature was held at about 200°C and the samples deposited at this temperature will be referred to as samples deposited onto a "hot substrate". The nominal thickness of the films deposited onto "hot substrate" was about 120 nm.

UV-Vis spectra of the films were recorded using a UV–Vis-3101PC ''Shimadzu'' spectrophotometer. IR spectra were recorded using a Vertex 80 FTIR spectrometer. Raman spectra were recorded with a LabRAM HR Evolution (Horiba) spectrometer in a back-scattering geometry. The 488 nm, 100 mW line of an Ar-laser was used for spectra excitation.

Crystalline structure studies were carried out using Bruker DUO single crystal diffractometer (4-circle kappa-goniometer, MoK_α sealed tube with graphite monochromator, Apex II CCD area-detector) using conventional phi- and omega-scans (0.5° wide). The sample temperature was kept at 155K using Oxford Cryosystem Cobra nitrogen open-flow cooler for all samples. Crystallographic data for these compounds have been deposited in the Cambridge Crystallographic Data Centre (CCDC) with reference numbers 1572908-1572911.

X-ray diffraction patterns for polycrystalline powders were obtained using Shimadzu XRD-7000 powder diffractometer (Cu-anode sealed tube, Bragg-Brentano geometry, θ-2θ goniometer, scintillation counter). Thin film samples were studied using combination of both mentioned above instruments: XRD-7000 for standard powder patterns and Bruker DUO (CuKα, Incoatec IμCu microfocus source, 1024x1024 pixel flat CCD detector) for 2D GIXD patterns using a special sample adaptor. The primary beam angle of incidence was in the range from 0.3 to 0.5°. Distance from the sample to the CCD detector was 80 mm. This method was described earlier in more details [17].

Additionally, the molecular structures and IR-spectrums of separate PdPc, PdPcF4 and PdPcF16 molecules were estimated with the density functional theory (DFT) using the BP86/def2-SVP method [18-21] and Grimme D3 dispersion correction [22-23]. The GAMESS suite of quantum chemical programs was used for these calculations [24] performed under symmetry constraints (D_{4h} for PdPc and $PdPcF_{16}$ and C_{4h} for $PdPcF_4$).

3. Results and discussion

3.1. Structure of single crystals of PdPc, PdPcF$_4$ and PdPcF$_{16}$

Optical images of PdPc, PdPcF$_4$ and PdPcF$_{16}$ single crystals are shown in Fig. 2. All three compounds formed needle-shaped crystals with dark violet color and metallic shine which is typical for unsubstituted and fluorinated phthalocyanines. PdPc formed relatively large freestanding blocks consisting of several single crystals about 0.5 mm in length. PdPcF$_4$ crystals grew as a dense layer of thin (less than 50μm in thickness) and long (up to 5mm) intersecting needles, while PdPcF$_{16}$ formed clusters of short needles on the top of a polycrystalline layer.
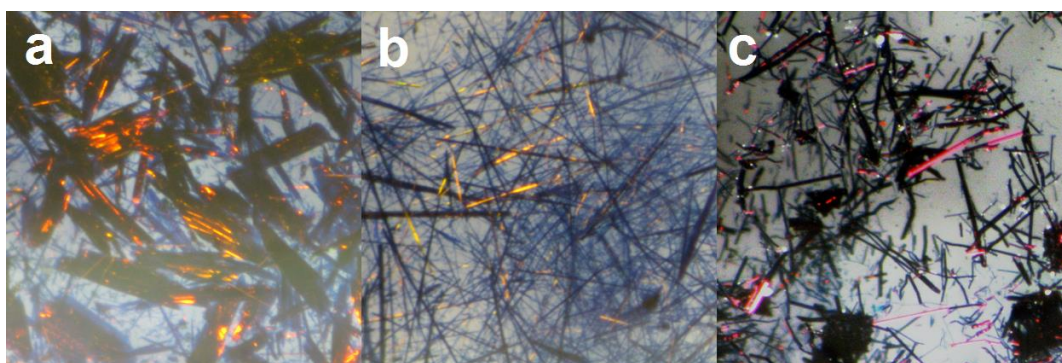

Figure 2. Microscopic images of PdPc (a), PdPcF$_4$ (b) and PdPcF$_{16}$ (c) crystals suspended in liquid epoxy.

X-ray diffraction patterns for PdPc, PdPcF$_4$ and PdPcF$_{16}$ polycrystalline powders were obtained using Shimadzu XRD-7000 powder diffractometer (Cu-anode sealed tube, Bragg-Brentano geometry, θ-θ goniometer, scintillation counter) in the 2θ range from 5 to 40° (Fig. S1, Supporting Information). PdPc and PdPcF$_4$ powders apparently consist of a single crystal phase, while PdPcF$_{16}$ powder contains at least two phases. However, upon closer investigation, it has been found that PdPc polycrystalline powder consists of two crystal phases, namely α-PdPc (small low-quality crystals), which are present in a larger amount and γ-PdPc (a few large, high-quality crystals). Fig. S2 shows "cake" images obtained from PdPc diffraction patterns using Dioptas 0.4.0 software [25]. Diffraction patterns of specially prepared samples (fine crystalline powder mixed with epoxy glue and rolled into 0.5mm balls) were obtained in Debye-Scherrer geometry using a Bruker DUO single-crystal diffractometer. This technique was described in details by Sukhikh et al. [17, 26]. Similar efforts have been made in order to find two different crystal

phases for $PdPcF_{16}$, however, all selected crystals were of the same phase (β-$PdPcF_{16}$), and no α-$PdPcF_{16}$ crystals suitable even for unit cell determination were found.

The crystal structures of all three compounds were determined by means of single crystal X-ray diffraction. The Bruker APEX II V2013.6-2 software package [27] was used for indexing, collecting raw data, integration of diffraction reflections and global unit cell refinement. For PdPc and $PdPcF_4$ absorption correction was applied using SADABS-2012/1, while for $PdPcF_{16}$ absorption correction was applied using TWINABS-2012/1, since the $PdPcF_{16}$ crystal turned out to be a perfect non-merohedral twin with 0.83/0.17 twin ratio, twinned by 180° rotation around (010) direction in direct cell. Fig S3 shows reciprocal lattice view for $PdPcF_{16}$ with two intersecting crystal domains. SHELXT-2014/5 [28] and SHELXL-2016/6 [28] were used for structure determination and subsequent refinement. All non-hydrogen atom positions were refined anisotropically, without additional constraints. For $PdPcF_4$, fluorine atoms occupancy was refined as free variable, based on the assumption that the total occupancy for two neighboring positions should be equal to unity. The resulting values are 0.521/0.479 and 0.562/0.438. Such noticeable deviation from 0.5 is apparently caused by uneven proportions of $PdPcF_4$ isomers in the initial product of synthesis. Hydrogen atoms were refined using aromatic/amide riding coordinates. Sample properties, details of data collection and structure refinement for all three phthalocyanine derivatives are given in Table 1.

Table 1. Summary of crystallographic data for α-PdPc, γ-PdPc, $PdPcF_4$ and $PdPcF_{16}$

Compound	α-PdPc	γ-PdPc	$PdPcF_4$	$PdPcF_{16}$
Formula	$Pd_1C_{32}N_8H_{16}$	$Pd_1C_{32}N_8H_{16}$	$Pd_1C_{32}N_8F_4H_{12}$	$Pd_1C_{32}N_8F_{16}$
F.W.	618.93	618.93	690.90	906.80
System	Monoclinic	Monoclinic	Triclinic	Triclinic
Space group	C2/c	P2$_1$/n	P-1	P-1
Z	4	2	1	2
a	26.105(8)	16.621(3)	3.6762(3)	6.8332(16)
b	3.7545(11)	3.8791(8)	12.2816(9)	14.987(3)
c	23.908(6)	18.045(4)	13.563(1)	15.667(4)
α	90	90	87.977(3)	64.335(7)

β	94.042(9)	95.736(5)	84.734(3)	80.727(8)
γ	90	90	85.308(3)	79.799(7)
Volume	2337.4(11)	1157.7(4)	607.52(8)	1416.8(6)
V/Z	584.4	578.9	607.52	708.4
Density (calc)	1.759	1.776	1.888	2.126
F(000)	1240	620	342	876
R_1 (I>2θ)	4.62%	3.20%	2.60%	4.79%
R_{w2}(I>2θ)	8.12%	6.27%	5.18%	10.88%
R_1 all	9.16%	5.41%	2.95%	8.82%
R_{w2} all	9.46%	6.90%	5.30%	12.01%

Individual molecules and packing diagrams are shown in Fig. 3. Internal macrocycles of all three molecules retain a virtually flat conformation with central metal atoms laying exactly on the mean square plane, and all carbon, nitrogen and fluorine atoms deviating out of plane no more than 0.1 Å for α-PdPc, β-PdPc and PdPcF$_{16}$, and 0.05 Å for PdPcF$_4$.
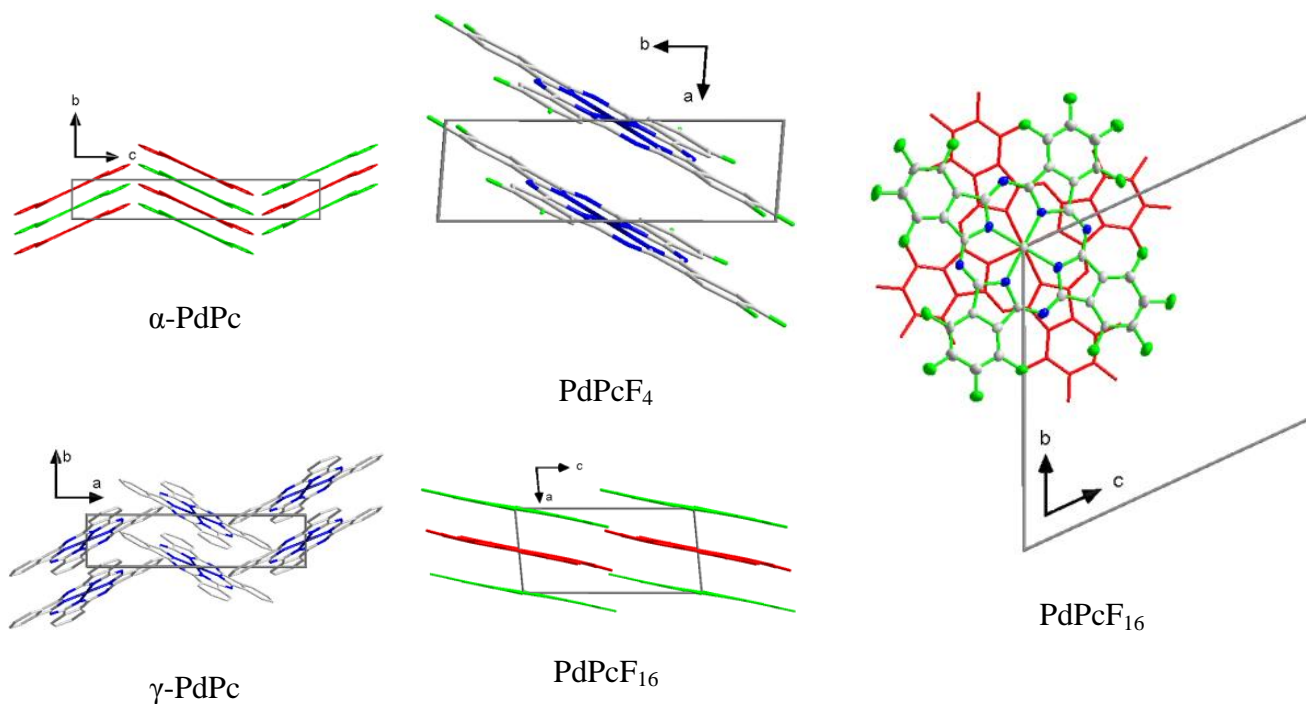

Figure 3. Packing diagrams for α-PdPc, γ-PdPc, PdPcF$_4$ and PdPcF$_{16}$

After comparing unit cell parameters and crystal structure it is clear that α-PdPc and γ-PdPc are isostructural to α-PtPc and γ-PtPc, respectively [29]. Molecules of α-PdPc are packed in stacks with herringbone arrangement (Z = 4, monoclinic system, C2/c space group). The distance between individual molecules within a stack is 3.416 Å (3.454 Å for α-PtPc), with adjacent stacks shifted by ½ of this distance, as shown in Fig. 3; the distance between neighboring Pd atoms is 3.755Å (3.818 Å for α-PtPc), which gives a packing angle θ = 24.53° (25.21° for α-PtPc). The crystal packing of α-PdPc differs from most α-M(II)Pcs (M=Cu, Co, Zn, Ni, H2) [8, 30] and is similar to PtPc [29]. The crystal packing of another phase of PdPc is similar to γ-PtPc [29]. γ-PdPc is packed in stacks with herringbone arrangement (Z = 2, monoclinic system, P21/n space group), however in this case the adjacent stacks are in line with one another. The distance between individual molecules within a stack is 3.366Å (3.412 Å for γ-PtPc) and the distance between neighboring Pd atoms is 3.879Å (3.969 Å for γ-PtPc), which gives a packing angle θ = 29.8° (30.73° for γ-PtPc).

PdPcF$_4$ molecules, on the other hand, are packed similarly to low-temperature metastable α-phases of Co(II)Pc (Z=1, triclinic system, P-1 space group) [30], with 3.373Å between individual molecules within a stack and 3.676 Å between neighboring Pd atoms, and θ = 23.45°. PdPcF$_4$ consists of columnarly arranged molecules; those of adjacent columns are aligned parallel to one another.

PdPcF$_{16}$ (Z=2, triclinic system, P-1 space group) has two molecules per unit cell, arranged almost in parallel (0.985° angle between mean square planes of both molecules) and rotated relative to each other in-plane for ca. 35.5°. Such an arrangement of molecules results in a packing similar to that of PdPcF$_4$, with ~3.23Å between molecules, 3.417 Å between neighboring Pd atoms and θ ~ 19°. The structure of single crystals of tetrafluorosubstituted metal phthalocyanines has not been determined until the present time, while the single crystal structures of MPcF$_{16}$ (M=Co, Cu, Zn) have been described by Jiang and co-workers [15]. However, the structure of PdPcF$_{16}$ single crystals differs from the known MPcF$_{16}$ structures.

Some intramolecular parameters of PdPc, PdPcF$_4$ and PdPcF$_{16}$ are given in Table 2, where values in the brackets were received by quantum-chemical calculations. It follows that average relative error of the

DFT method here is low and does not exceed 2.3%, what allows us to get satisfactory results of IR-spectrums calculations further.

3.2. Thin Films of PdPc, PdPcF$_4$ and PdPcF$_{16}$

3.2.1. X-ray diffraction study

It is known that the choice of deposition conditions might affect significantly the growth process and molecular organization of thin organic films. Significant efforts have been made so far towards the development of growth methods and, ultimately, to control the molecular structure (e.g., molecular orientation, polymorphism, and morphology) of the MPc films [31, 32]. Among the large variety of factors that contribute to the films' morphology, the substrate temperature during film growth has been reported to modify the structure of the studied MPc films [30, 33].

X-ray diffraction patterns of thin films of PdPc, PdPcF$_4$ and PdPcF$_{16}$ deposited onto cold and hot substrates, obtained in the 2θ range from 2.5 to 30° are shown in Fig. 4.

Table 2. Bond lengths (Å) in PdPc, PdPcF$_4$ and PdPcF$_{16}$ molecules. Bond lengths (Å) in the brackets were received by quantum-chemical calculations.

Bond	γ-PdPc	PdPcF$_4$	PdPcF$_{16}$
Pd-N$_\alpha$	1.979 (2.004)	1.974 (2.004)	1.973 (2.006)
N$_\alpha$-C$_\alpha$	1.375 (1.382)	1.373 (1.382)	1.378 (1.381)
C$_\alpha$-N$_\beta$	1.332 (1.329)	1.328 (1.329)	1.318 (1.327)
C$_\alpha$-C$_\beta$	1.464 (1.466)	1.456 (1.467)	1.459 (1.464)
C$_\beta$-C$_\beta$	1.400 (1.420)	1.396 (1.420)	1.400 (1.425)
C$_\beta$-C$_\gamma$	1.392 (1.402)	1.392 (1.401)	1.384 (1.401)
C$_\gamma$-C$_\delta$	1.389 (1.405)	1.376 (1.401)	1.381 (1.410)
C$_\delta$-C$_\delta$	1.405 (1.415)	1.392 (1.412)	1.385 (1.414)
C-H	0.950 (1.100)	0.950 (1.099)	-
C$_\gamma$-F	-	-	1.351 (1.332)
C$_\delta$-F	-	1.331 (1.437)	1.347 (1.335)

Diffraction patterns of all films contain one strong diffraction peak in the range of 6-7° and several low intense peaks ($I/I_{max} < 5\%$). This fact together with the fact that majority of the observed diffraction peaks have aliquot interplanar spacings (i.e. $d = n$, $n/2$, $n/3$, $n/4$ etc.) suggests that all six samples have strong preferred orientation. Crystal phase composition of the films can be determined by comparing interplanar spacings of the observed diffraction peaks with the values calculated from the crystal structure data. PdPc films deposited both on cold and hot substrates consist of α-phase with strong preferred orientation along (200) plane. The diffraction pattern of the sample deposited on a hot substrate, however, also contains the (002) peak, which points to either decreased degree of ordering or second preferred orientation along (002) plane. All diffraction peaks on the pattern of the film deposited on the hot substrate have significantly lower FWHM values compared to that deposited on the cold substrate, which is apparently caused by the increased size of individual crystallites.
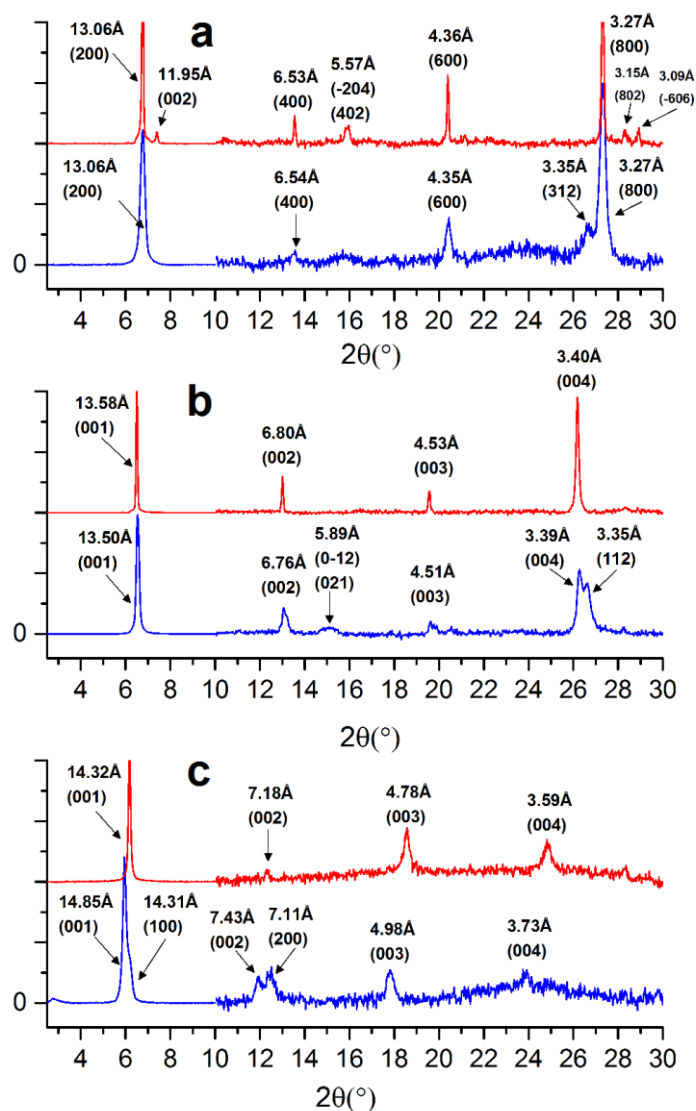
Figure 4. X-ray diffraction patterns of thin films of PdPc (a), $PdPcF_4$ (b) and $PdPcF_{16}$ (c), deposited on cold (blue lines) and hot (red lines) substrates.

$PdPcF_4$ films deposited on cold and hot substrates grow in the same crystal phase as its polycrystalline powder and single crystals. Both films have preferred orientation along (001) plane, however the diffraction pattern of the film deposited on a hot substrate consists of only diffraction peaks with (00l) indexes with much lower FWHM and much higher intensities compared to that deposited on a cold substrate, indicating that $PdPcF_4$ film on a hot substrate has more ideal orientation.

$PdPcF_{16}$ samples, on the other hand, show significant differences between the two diffraction patterns. While films deposited on a hot substrate consist of β-phase perfectly oriented along the (001) plane, films

deposited on a cold substrate consist of α-phase with unknown crystal structure and unit cell parameters. By analogy with $PdPcF_4$, the indices (001) and (100) were assigned to the first two diffraction peaks on the diffraction pattern of $PdPcF_{16}$ deposited on a cold substrate. Since the four remaining diffraction peaks have interplanar distances that are natural fractions of the first two peaks, the corresponding indexes (002, 003, 004 and 200) were assigned to them.

X-ray diffraction studies of thin films in 2D GIXD geometry were carried out for further detailed investigation of the films structure (Fig. 5). In all cases a 2θ position of the detector was equal to zero, i.e. the zero point of the diffraction pattern coincides with the center of the detector. Since the left halves of each 2D GIXD pattern were shadowed by the substrate material, only the right halves of the diffraction patterns are shown.
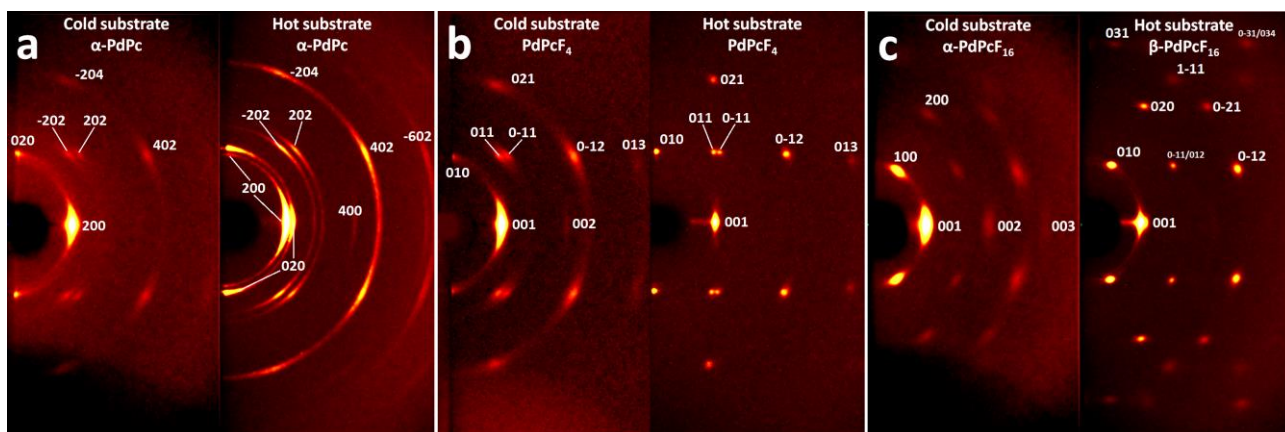

Figure 5. 2D GIXD patterns for the film of PdPc (a), $PdPcF_4$ (b) and $PdPcF_{16}$ (c), deposited on cold (left image) and hot (right image) substrates.

Appearance of 2D GIXD patterns confirms the assumptions made earlier about the phase composition and preferred orientation of each sample. Using the available structural data, the corresponding Miller indices were attributed to all of the observed diffraction spots. 2D GIXD pattern of PdPc film deposited on a hot substrate shows (200) and (002) peaks in the middle, confirming that the film has two competing preferred orientations. Significant reduction in the size of the diffraction spots in $PdPcF_4$ and $PdPcF_{16}$ patterns indicates a greatly increased degree of ordering in both samples deposited on hot substrates. It is

worth mentioning that the patterns of $PdPcF_{16}$ film deposited on a cold substrate is visually similar to that deposited on a hot substrate, suggesting that the unit cell parameters of both $PdPcF_{16}$ phases must be close to one another.

Knowledge of the crystalline structures and preferred orientations for α-PdPc, $PdPcF_4$ and $PdPcF_{16}$ films will allow the calculation of the angle between the phthalocyanine macrocycles and substrate surface. The inclination angle of PdPc molecules is 86.8° in the films deposited on cold substrates, while two angles (86.8° and 65.5°) are observed in the case of PdPc films deposited on hot substrates; the latter is caused by the presence of two different preferred crystallites orientations. The inclination angle of $PdPcF_4$ molecules is 89.5° for both films deposited on cold and hot substrates, whereas two inclination angles of 75.90° and 75.01° are observed for molecules in $PdPcF_{16}$ films deposited on hot substrates. This is due to the occurrence of two independent molecules in $PdPcF_{16}$ structure, which are not exactly parallel to each other. The scheme of orientation of molecules in palladium phthalocyanine relative to the substrate surface is given in Fig. S4.

Additional information about the degree of films orientation can be obtained by measuring azimuthal profiles of diffraction spots in 2D GIXD patterns and then measuring their FWHM, since the azimuthal profile of a diffraction spot effectively shows the distribution of the slope angle of the corresponding crystallographic plane relative to the substrate surface. The most intense peaks on each pattern (peaks 200 for both PdPc samples, peaks 001 for $PdPcF_4$ and $PdPcF_{16}$) were selected and their profiles were integrated in the range ±0.3° from their 2θ maximum (since all selected peaks have FWHM $\approx 0.3°$, the 0.6° wide band would contain most of the diffraction peak). Fig. 6 shows azimuthal profiles for the films deposited on cold (black lines) and hot (red lines) substrates.
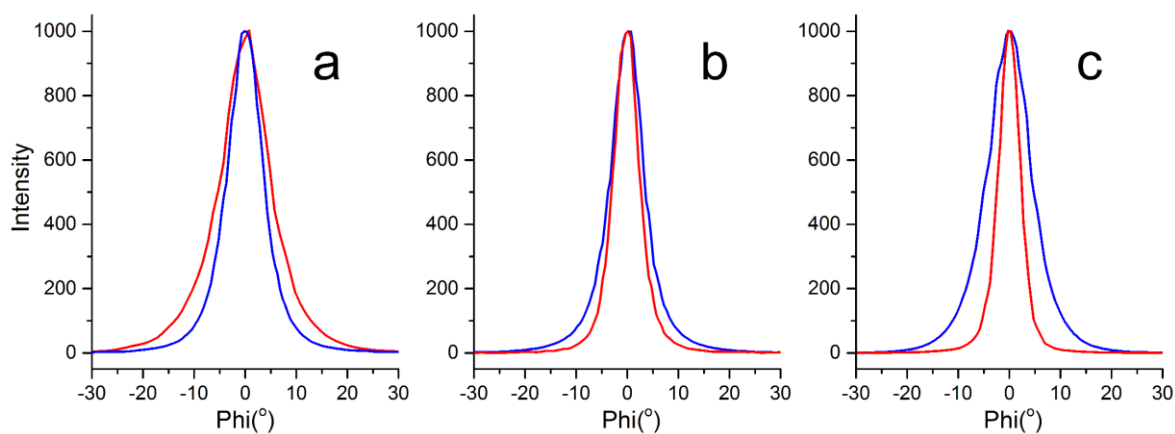
Figure 6. Azimuthal profiles for the most intense peaks on 2D GIXD patterns of thin films of PdPc (a), PdPcF$_4$ (b) and PdPcF$_{16}$ (c), deposited on cold (blue lines) and hot (red lines) substrates.

It can be clearly seen that PdPc thin films deposited on hot substrates are less oriented (FWHM = 8.09° for a cold substrate and 11.20° for a hot substrate) while PdPcF$_4$ and PdPcF$_{16}$ films significantly increase their degree of ordering (FWHM changes from 7.41° to 5.78° for PdPcF$_4$ and from 10.04° to 4.93° for PdPcF$_{16}$).

3.2.1. Spectral study

Optical properties of phthalocyanine films are also sensitive to their structural features, especially to their polymorphic modifications [34, 35]. Fig. 7 shows the electronic absorption spectra of PdPc, PdPcF$_4$ and PdPcF$_{16}$ films deposited on cold and hot substrates. In the spectra of all films the Q-bands are significantly broader than in the spectra of solutions.
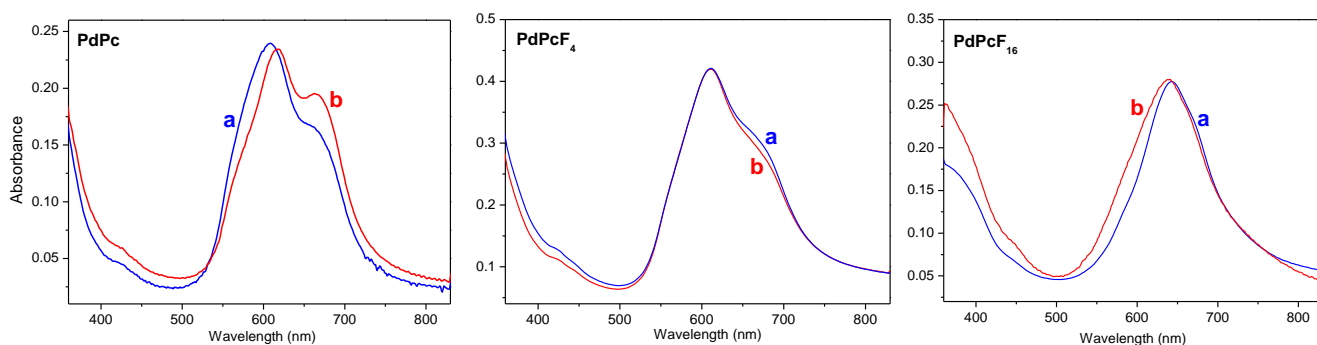

15

Figure 7. Optical absorption spectra of PdPc, PdPcF$_4$ and PdPcF$_{16}$ films, deposited on cold (a) and hot substrates

The Q-band in the UV-Vis spectra of the PdPc film deposited on a cold substrate splits into two bands with maxima at 609 and 662 nm, while these bands lie at 619 and 665 in the case of film deposited on a hot substrate. The splitting of the Q-band in the films' spectra is explained in terms of factor group splitting and arises from exciton coupling between two non-equivalent molecules in a unit cell [36]. It has been shown by XRD that both PdPc films consist of α-phase with preferred orientation along (200) plane and differ only by the degree of ordering.

Optical absorption spectra of PdPcF$_4$ deposited on cold and hot substrates are similar; the Q-band in the UV-Vis spectrum of the PdPcF$_4$ films has a maximum at 611 with a small shoulder at 668 nm. The films of PdPcF$_{16}$ exhibit a Q-band with one maximum at 643 nm in the case of deposition on a cold substrate and at 638 nm in the case of deposition on a hot substrate. Such spectra with an un-splitting Q band are usually observed for films with a co-facial parallel arrangement of chromophores [37-38].

Vibrational spectroscopy methods have also been used to complement XRD methods to distinguish types of molecules packing in MPcs of different phases [39-40]. The first investigation of Raman spectra of MPc polymorphs has been carried out by Aroca and co-workers in 1982 [41-42].

The assignment of the bands in the vibrational spectra of PdPc and PdPcF$_{16}$ has already been published in our previous work [16], however, the vibrational spectra of PdPcF$_4$ derivative have not been discussed in the literature. The experimental and DFT calculated IR spectra of the studied PdPc forms are presented in Fig. 8. A comparison of the experimental and calculated bands in the IR and Raman spectra of their assignments is given in Tables S1-S2 (Supplementary Information). The experimentally measured vibrational wavenumbers of all molecules coincide well with DFT theoretical predictions. The RMS difference between the calculated and experimental wavenumbers was 20 cm^{-1}. The IR spectra of all three derivatives are presented in Fig. S5.
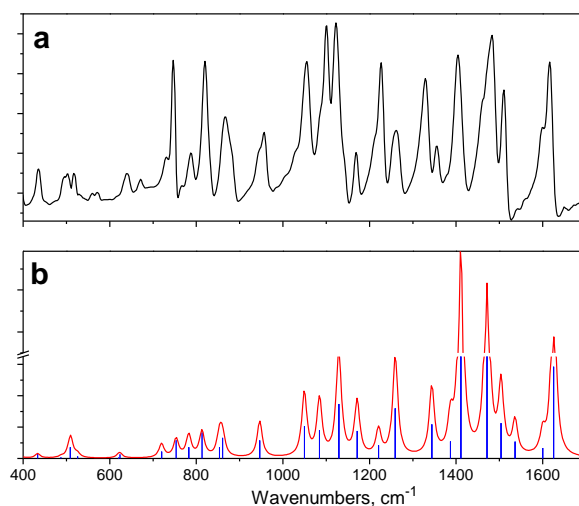
Figure 8. Experimental (a) and DFT calculated (b) IR spectra of $PdPcF_4$.

Introduction of electron withdrawing F-substituents causes the change of both position and intensities of most of the vibrations in the vibrational spectra. The group of fundamentals dominated by macro ring breathing and $Pd-N_\alpha$ in-plane stretching vibrations lie in the range of 500-650 cm^{-1}. Another group of vibrations at 760-800 cm^{-1} is attributed to the $N_\alpha-C_\alpha-N_\beta$ and $C_\alpha-C_\beta-C_\beta$ deformations along with stretching of $Pd-N_\alpha$. The vibrations in the range of 1100-1160 cm^{-1} assigned to $C_\beta-C_\gamma-H$ deformation coupled with $C_\alpha-N_\alpha$ in-plane vibrations are observed in the spectra of PdPc and $PdPcF_4$. The position and intensities of the vibrations in the range from 1200 to 1360 cm^{-1} involving isoindole and pyrrole deformations in the spectrum of $PdPcF_4$ and $PdPcF_{16}$ differ from those of PdPc due to the high contribution of C-F stretching vibrations (Table S1). Introduction of F-substituents also causes the shift of C=C stretching vibrations to the longer-wave spectral region (1609 cm^{-1} for PdPc, 1616 cm^{-1} for $PdPcF_4$ and 1623 cm^{-1} for $PdPcF_{16}$ in the IR spectra). Raman spectra of the films of PdPc, $PdPcF_4$ and $PdPcF_{16}$ deposited on cold and hot substrates are given in Fig. 9.
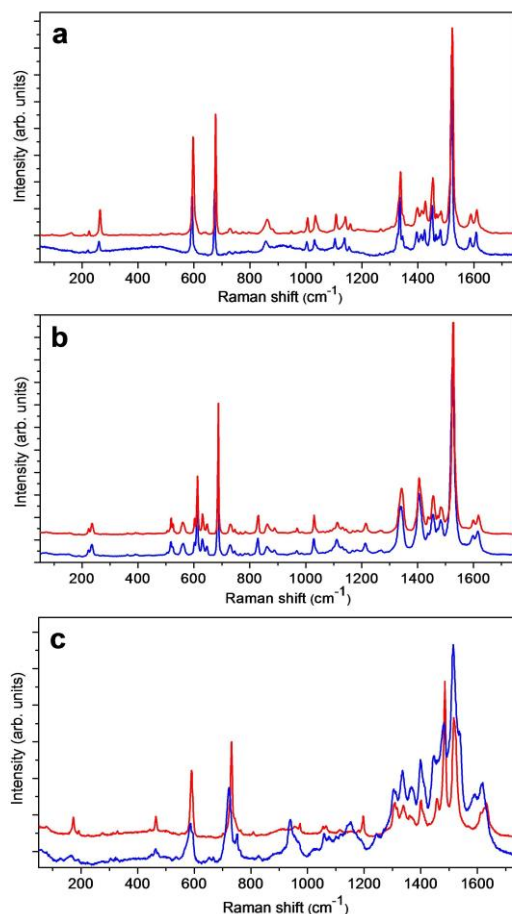
17

Figure 9. Raman spectra of PdPc (a), PdPcF$_4$ (b) and PdPcF$_{16}$ (c) films deposited on cold (blue lines) and hot (red lines) substrates

Raman spectra of PdPc and PdPcF$_4$ films deposited on cold (a) and hot (b) substrates are almost the same because these films deposited at different substrate temperatures have the same phase composition. In contrast, the Raman spectra of PdPcF$_{16}$ films have noticeable differences manifested mainly as a change of relative intensities of some vibrations. The most pronounced differences are observed in the spectral ranges 900-980 cm^{-1} and 1090-1200 cm^{-1}. The fundamentals in these spectral region (e.g. 954, 1120, 1180 cm^{-1}) are characterized by high contribution of C-F stretching vibrations [16]. It is not surprising that the end C-F groups are sensitive to the change of molecular packing. The stretching vibrations of C=C (1590-1640 cm^{-1}) in benzene rings of PcPcF$_{16}$ molecule are also quite sensitive to the change of the molecular packing. The modes below 200 cm^{-1} belonging to the lattice vibrations [43] are also dependent

on phase composition and molecular packing. The bands at 57, 127, 163 cm^{-1} are observed in the spectrum of PdPcF$_4$ films deposited on a cold substrate, whereas in the case of the film deposited on a hot substrate these bands are located at 52, 78, 173 cm^{-1}. It has been shown above by XRD methods that PdPcF$_{16}$ films deposited on a hot substrate consist of β-phase perfectly oriented along the (001) plane, while the films deposited on a cold substrate consist of α-phase with unknown crystal structure and unit cell parameters, that makes a detailed interpretation of the observed spectral distinctions more difficult. The optical properties of thin phthalocyanine films are determined by the polymorphic modification and molecular orientation in the film as discussed above. Similar effect of the structural features of PdPc films on the spectral properties was studied by Jafari et al. [7]. The structure and orientation of molecules in MPcs films are of particular importance for electronic device applications [2] and therefore detailed study of the structure of the films of palladium phthalocyanine derivatives can be quite valuable for the interpretation of films electrical data.

Conclusions

Effect of fluorination on the single crystal structure, molecular orientation and optical spectra of thin films of palladium phthalocyanine derivatives has been investigated. It has been shown that fluorination leads to the change of the structure of PdPcF$_4$ and PdPcF$_{16}$ compared to unsubstituted PdPc. Crystalline structures of single crystals of unsubstituted PdPc, its tetrafluorinated and hexadecafluorinated derivatives grown by vacuum sublimation have been determined by X-ray diffraction. Two phases have been identified for PdPc, both crystallize in stacks with herringbone molecular arrangement in the monoclinic space groups; α-PdPc in C2/c; and γ-PdPc in P2$_1$/n. Both PdPcF$_4$ and PdPcF$_{16}$ are shown to crystallize in the triclinic P-1 space group, forming stacks of molecules in columnar arrangement. Stacks of molecules in adjacent columns are aligned parallel to one another; the unit cell parameters of PdPcF$_4$ are Z=1, a=3.6762(3), b= 12.2816(9), c= 13.563(1), α=87.977(3)$^{\mathrm{o}}$, β=84.734(3)$^{\mathrm{o}}$, γ=85.308(3)$^{\mathrm{o}}$, while those of PdPcF$_{16}$ are Z=2, a=6.8332(16), b= 14.987(3), c= 15.667(4), α=64.335(7)$^{\mathrm{o}}$, β=80.727(8)$^{\mathrm{o}}$, γ=79.799(7)$^{\mathrm{o}}$.

Thin films of F-substituted PdPc grown by organic molecular beam deposition at different substrate temperatures were also shown to exhibit structural, molecular orientation and spectral feature changes. Structure and molecules orientation in MPcs films are known to be of particular importance for electronic device applications. It has been shown that PdPc films deposited both on cold and hot substrates consist of α-phase. The inclination angle of PdPc molecules is 86.8° in films deposited on cold substrates, while two angles (86.8° and 65.5°) are observed in the case of PdPc films deposited on hot substrates due to the occurrence of two different molecular preferred orientations.

$PdPcF_4$ films deposited on cold and hot substrates grow in the same crystal phase as its polycrystalline powder and single crystals. Both films have preferred orientation along (001) plane; the inclination angle of $PdPcF_4$ molecules relative to the substrate surface is 89.5° for both films. $PdPcF_{16}$ films deposited on a hot substrate consist of β-phase preferably oriented along the (001) plane, while the films deposited on a cold substrate consist of α-phase with unknown crystal structure and unit cell parameters. The inclination angles of $PdPcF_{16}$ molecules are 75.90°/75.01° for films deposited onto hot substrates. The obtained data can be used as a basis for the interpretation of films electrical data in future work.

References

[1] McKeown NB.Applications of Phthalocyaninei. In: Kadish KM, Smith R, Guilard R, editors. The Porphyrin Handbook. Academic Press; 15, San Diego CA; 2003, p.61-124.

[2] Kim I, Haverinen HM, Wang Z, Madakuni S, Li J, Jabbour GE. Effect of molecular packing on interfacial recombination of organic solar cells based on palladium phthalocyanine and perylene derivatives. Appl Phys Lett 2009;95:023305.

[3] Signerski R, Jarosz G, Koscielska B. On photovoltaic effect in hybrid heterojunction formed from palladium phthalocyanine and titanium dioxide layers. J Non-Crystalline Solids 2009;355:1405-1407.

[4] Jarosz G. On small signal capacitance spectra of organic diode formed by ITO–palladium phthalocyanine–Al sandwich system. Thin Solid Films 2010;518:4015-4018.

[5] Jafari MJ, Azim-Araghi ME, Barhemat S. Effect of chemical environments on palladium phthalocyanine thin film sensors for humidity analysis. J Mater Sci 2012;47:1992-1999.

[6] Azim-Araghi ME, Karimi-Kerdabadi E, Jafari MJ. Optical and electrical properties of nanostructured heterojunction (Au|PdPc|ClAlPc|Al) and using as O_2 sensor. Eur Phys J Appl Phys 2011;55:30203-30211.

[7] Jafari MJ, Azim-Araghi ME, Barhemat S, Riyazi S. Effect of post deposition annealing on surface morphology and gas sensing properties of palladium phthalocyanine thin films. Surf Interface Anal 2012;44:601-608.

[8] Engel MK. Single-Crystal Structures of Phthalocyanine Complexes and Related Macrocycles. In: Kadish KM, Smith R, Guilard R, editors. The Porphyrin Handbook; 20, San Diego CA; 2003, p.1-242.

[9] Iwatsu F, Kobayashi T, Ueda N. Solvent effects on crystal growth and transformation of zinc phthalocyanine. J Phys Chem 1980;84:3223-3230.

[10] Brown CJ. Crystal structure of β-copper phthalocyanine. J Chem Soc A 1968;10:2488-2493

[11] Tang Q, Li H, Liu Y, Hu W. High-Performance Air-Stable n-Type Transistors with an Asymmetrical Device Configuration Based on Organic Single-Crystalline Submicrometer/Nanometer Ribbons. J Am Chem Soc 2006; 128:14634-14639.

[12] de Oteyza DG, Barrena E, Osso JO, Sellner S, Dosch H. Thickness-dependent structural transitions in fluorinated copper-phthalocyanine (F16CuPc) films. J Am Chem Soc 2006;128:15052.

[13] Yoon SM, Song HJ, Hwang IC, Kim KS, Choi HC. Single crystal structure of copper hexadecafluorophthalocyanine, (F_{16}CuPc) ribbon. Chem Commun 2010;46:231–233.

[14] Pandey PA, Rochford LA, Keeble DS, Rourke JP, Jones TS, Beanland R, Wilson NR. Resolving the Nanoscale Morphology and Crystallographic Structure of Molecular Thin Films: $F_{16}CuPc$ on Graphene Oxide. Chem Mater 2012;24:1365−1370.

[15] Jiang H, Ye J, Hu P, Wei F, Du K, Wang N, Ba T, Feng S, Kloc C. Fluorination of Metal Phthalocyanines: Single-Crystal Growth, Efficient N-Channel Organic Field-Effect Transistors, and Structure-Property Relationships. Sci Reports 2014;4:7573.

[16] Parkhomenko RG, Sukhikh AS, Klyamer DD, Krasnov PO, Gromilov SA, Kadem B, Hassan AK, Basova TV. Thin films of unsubstituted and fluorinated palladium phthalocyanines: structure and sensor response toward ammonia and hydrogen. J Phys Chem C 2017;121(2): 1200–1209.

[17] Sukhikh AS, Basova TV, Gromilov, SA. Development of a procedure of X-ray study of thin layers by the example of cobalt phthalocyanine. Journal of Structural Chemistry;57 (3):618-621.

[18] Becke AD. Density-functional exchange energy approximation with correct asymptotic behavior. Phys Rev A 1988;88:3098-3100.

[19] Perdew JP. Density functional approximation for the correlation energy of the inhomogeneous electron gas. Phys Rev B 1986;33:8822-8824.

[20] Schaefer A, Horn H, Ahlrichs R. Fully optimized contracted Gaussian basis set for atoms Li to Kr. J Chem Phys 1992;97:2571-2577.

[21] Schaefer A, Huber C, Ahlrichs R. Fully optimized contracted Gaussian basis set of triple zeta valence quality for atoms Li to Kr. J Chem Phys 1994;100:5829-5835.

[22] Grimme S, Ehrlich S, Goerigk L. Effect of the Damping Function in Dispersion Corrected Density Functional Theory. J Comput Chem 2011;32:1456-1465.

[23] Grimme S, Antony J, Ehrlich S, Krieg H. A consistent and accurate ab initio parametrization of density functional dispersion correction (DFT-D) for the 94 elements H-Pu. J Chem Phys 2010;132:154104.

[24] Schmidt MW, Baldridge KK, Boatz JA, Elbert ST, Gordon MS, Jensen JH, et al. General atomic and molecular electronic structure system. J Comput Chem 1993;14(11):1347-1363.

[25] Prescher C, Prakapenka VB. DIOPTAS: a program for reduction of two-dimensional X-ray diffraction data and data exploration. High Pressure Research 2015;35(3):223-230.

[26] Sukhikh AS, Basova TV, Gromilov SA. Thin Layers XRD Study Technique on an Example of Cobalt Tetrafluoro Phthalocyanine. Acta Phys Polonica A 2016;130:889-891.

[27] Bruker Advanced X-ray Solutions, Madison, Wisconsin, USA.

[28] Sheldrick G.M. Crystal structure refinement with SHELXL. Acta Crystallogr C Struct Chem 2015;A71:3-8.

[29] Brown CJ. Crystal Structure of Platinum Phthalocyanine: A Re-investigation. J Chem Soc A 1968;0:2494-2498.

[30] Ballirano P, Caminiti R, Ercolani C, Maras A, Orru MA. X-ray Powder Diffraction Structure Reinvestigation of the α and β Forms of Cobalt Phthalocyanine and Kinetics of the $\alpha\rightarrow\beta$ Phase Transition. J Am Chem Soc 1998; 120:12798-12807.

[31] Zhu S, Banks CE, Frazier DO, Penn B, Abdeldayem H, Hicks R, Burns HD, Thompson GW. Structure and morphology of phthalocyanine films grown in electrical fields by vapor deposition. J. Cryst. Growth 2000;211:308-312.

[32] Basova T, Kiselev V, Dubkov I, Latteyer F., Gromilov S, Peisert H, Chassé T. Optical Spectroscopy and XRD Study of Molecular Orientation, Polymorphism, and Phase Transitions in Fluorinated Vanadyl Phthalocyanine Thin Films. J Phys Chem C 2013;117:7097-7106.

[33] Schuster B, Basova T, Plyashkevich V, Peisert H, Chassé T. Effects of temperature on structural and morphological features of CoPc and CoPcF$_{16}$ thin films. Thin Solid Films 2010;518:7161-7166.

[34] El-Nahassa MM, El-Goharyb Z, Solimana HS. Structural and optical studies of thermally evaporated CoPc thin films. Optics Laser Technol 2003;35:523-531.

[35] Fujita K, Muto J, Itoh KM. Morphological, electrochemical and optical properties of heat-treated magnesium phthalocyanine films. J Mater Sci Lett 1997;16:1894-1897.

[36] Kasha M, Rawls HR, El-Bayoumi MA. The excition model in molecular spectroscopy. Pure Appl Chem 1965;11:371-392.

[37] Schlettwein D, Hesse K, Tada H, Mashiko S, Storm U, Binder J. Ordered Growth of Substituted Phthalocyanine Thin Films: Hexadecafluorophthalocyaninatozinc on Alkali Halide (100) and Microstructured Si Surfaces. Chem Mater 2000;12: 989-995.

[38] Schlettwein D, Graaf H, Meyer JP, Oekermann T, Jaeger NI. Molecular Interactions in Thin Films of Hexadecafluorophthalocyaninatozinc (F_{16}PcZn) as Compared to Islands of N,N'-Dimethylperylene-3,4,9,10-biscarboximide (MePTCDI). J Phys Chem B 1999;103:3078-3086.

[39] Sauvage FX, de Backer MG, Stymne B. An infrared study of the complexing ability of manganese phthalocyanine. Spectrochim Acta 1982;38A:803-809.

[40] Menzel ER, Jordan KL. Fluorescence of solid metal-free phthalocyanine. Chem Phys 1978;32:223-229.

[41] Aroca R, DiLella DP, Loutfy RO. Raman Spectra of Solid Films: I. Metal-Free Phthalocyanine. J Phys Chem Solids 1982;43:707-711.

[42] Aroca R, Loutfy RO. Enhanced Raman scattering from molecular-dye films on silver. J Raman Spectrosc 1982;12:262-265.

[43] Basova TV, Kolesov BA. Raman Polarization Studies of Orientation of molecular thin films. Thin Solid Films. 1998;325:140-144.